A PHASE COMPENSATION ALGORITHM FOR HIGH-RESOLUTION PULSE RADAR SYSTEMS

Takuya SAKAMOTO and Toru SATO

Department of Communications and Computer Engineering

Graduate School of Informatics Kyoto University

Yoshida-Honmachi, Sakyo-ku, Kyoto, 606-8501, Japan

E-mail t-sakamo@aso.cce.i.kyoto-u.ac.jp

1. Introduction

Many studies have been done to develop high-resolution algorithms for pulse radar systems [1–7], which can be applicable for many kind of applications including rescue robots. High-resolution algorithms utilize not only the envelope of the received signal but also the phase of carrier signal. However, it should be noted that the received carrier phase depends on the shape of targets. Especially, $\pi/2$ phase rotation caused by concave is well-known in the field of electric-magnetic wave theory. The effect has not been regarded as a serious problem so far for pulse radar systems, because conventional systems having a narrow bandwidth do not deal with the accuracy. However, in the near future, the problem will become a bottleneck in improving the accuracy of pulse radar systems. In this paper, we propose an algorithm to compensate for the phase rotation caused by the concave and show an application example [8]. The algorithm is presented firstly, which is followed by numerical simulations for validation of the algorithm.

2. System Model

We assume a mono-static radar system in this paper. An omni-directional antenna is scanned along a straight line. UWB pulses are transmitted at a fixed interval and received by the antenna. The received data is A/D converted and stored in a memory. We estimate target shapes using the data.

We deal with a 2-dimensional problem, and TE-mode wave. Targets and the antenna are located on a plane. We assume that each target has a uniform complex permittivity, and surrounded by a smooth boundary. We assume the medium of direct path is vacuum for simplicity. We define r-space as the real space, where targets and the antenna are located. We express r-space with the parameter (x, y). Both x and y are normalized by λ, which is the center wavelength of the transmitted pulse in a vacuum. We assume $y > 0$ for simplicity. The antenna is scanned along x-axis in r-space. We define $s'(X, Y)$ as the received electric field at the antenna location $(x, y) = (X, 0)$, where we define Y with time t and speed of the light c as $Y = ct/(2\lambda)$. We apply a matched filter of transmitted waveform for $s'(X, Y)$. We define $s(X, Y)$ as the output of the filter. We define d-space as the space expressed by (X, Y). We normalize X and Y by λ and the center period of transmitted waveform, respectively. The transform from d-space to r-space corresponds to imaging which we deal with in this paper.

3. SEABED Algorithm

We have already developed a non-parametric shape estimation algorithm based on BST (Boundary Scattering Transform) [9]. We call the algorithm SEABED (Shape Estimation

Algorithm based on BST and Extraction of Directly scattered waves). The algorithm utilizes the existence of a reversible transform BST between target shapes and pulse delays. Boundary Scattering Transform (BST) is expressed as

$$X = x + y\mathrm{d}y/\mathrm{d}x, \tag{1}$$

$$Y = y\sqrt{1 + (\mathrm{d}y/\mathrm{d}x)^2}, \tag{2}$$

where (X, Y) is a point on a quasi wavefront. (x, y) is a point on target boundary [9]. We have clarified that the inverse transform of BST is given by

$$x = X - Y\mathrm{d}Y/\mathrm{d}X, \tag{3}$$

$$y = Y\sqrt{1 - (\mathrm{d}Y/\mathrm{d}X)^2}, \tag{4}$$

where we assume $|\mathrm{d}Y/\mathrm{d}X| \leq 1$. We call the transform in Eq. (3) and (4) Inverse Boundary Scattering Transform (IBST).

First, we extract a quasi wavefront from $s(X, Y)$ in SEABED. Quasi wavefronts have to satisfy the condition $\mathrm{d}s(X, Y)/\mathrm{d}Y = 0$ and $|\mathrm{d}Y/\mathrm{d}X| \leq 1$. Furthermore, we adopt a condition $|s(X_i, Y_i)/s(X_{i+1}, Y_{i+1})| < T_\mathrm{r}$ to prevent an interference, where (X_i, Y_i) and (X_{i+1}, Y_{i+1}) are points on a quasi wavefront and next to each other. Next, we apply IBST to the extracted quasi wavefront and estimate the target shape.

Fig. 1 shows an example of target boundary surface. Fig. 2 shows the received data from the assumed target. We obtain this signal by utilizing FDTD (Finite Difference Time Domain) method. We receive the signal at the 39 locations whose intervals are 0.125λ. Next, we extract quasi wavefronts using the conditions mentioned in the previous subsection. We adopt an empirically chosen value $T_\mathrm{r} = 1.11$. The extracted quasi wavefronts are shown in Fig. 3. Five quasi wavefronts are extracted in the figure. Fig. 4 shows the estimated target boundary surfaces using the SEABED. The solid line and the broken lines are the real target boundary surface and the estimated target boundary surfaces, respectively. The estimation accuracy on the concave surface suffers degradation compared to the straight surface. This is caused by the phase rotation occurred at the caustic to the echoes from the concave surface [10]. Here, physically singular points are called caustics.

4. Phase Compensation for IBST

The phase rotation depends on the shape of target. It is possible to compensate for the phase rotation if the condition of phase rotation can be expressed using the extracted quasi wavefronts. Eq. (3) and Eq. (4) are expressed as

$$\begin{bmatrix} x \\ y \end{bmatrix} - \begin{bmatrix} X \\ 0 \end{bmatrix} = \boldsymbol{v}_\mathrm{IBST}, \quad \boldsymbol{v}_\mathrm{IBST} = \begin{bmatrix} -Y\mathrm{d}Y/\mathrm{d}X, \\ Y\sqrt{1 - (\mathrm{d}Y/\mathrm{d}X)^2} \end{bmatrix}, \tag{5}$$

where we define the IBST vector $\boldsymbol{v}_\mathrm{IBST}$.

The caustic curve $(x_\mathrm{f}, y_\mathrm{f})$ of a target boundary satisfies

$$\begin{bmatrix} x_\mathrm{f} \\ y_\mathrm{f} \end{bmatrix} - \begin{bmatrix} X \\ 0 \end{bmatrix} = \tan\phi\boldsymbol{v}_\mathrm{IBST}, \tag{6}$$

where ϕ is defined as

$$\phi = \tan^{-1}\left\{ \frac{1 - (\mathrm{d}Y/\mathrm{d}X)^2}{Y\mathrm{d}^2Y/\mathrm{d}X^2} \right\}. \tag{7}$$

We see that a caustic is on the line which connects the antenna and the boundary. ϕ is the parameter which shows the relative position of the caustic for the antenna. The relationship

between ϕ and target shapes is shown in Fig. 5, where we see that $0 < \phi < \pi/4$ is the condition for $\pi/2$ phase rotation. We can directly detect a caustic and antenna position with quasi wavefronts utilizing ϕ.

5. An Application Example of the Phase Compensation Algorithm

Fig. 6 shows a calculated ϕ for each quasi wavefront. The calculated ϕ is plotted with X in the figure. Calculated ϕ are located in the correct region for quasi wavefronts "2" and "5". On the other hand, edge diffraction "3" and "4" have ϕ around $\pi/4$, which means it is close to a point target. As for quasi wavefront "1", calculated ϕ is about $\pi/8$ at the center, but the both ends has wrong ϕ in the convex region. First, we calculate the average ϕ for each quasi wavefront. Next, we determine phase compensation using the averaged ϕ. We set margin for the threshold to make the algorithm stable. We adopt empirically chosen condition $5° < \phi < 40°$ for phase compensation. Fig. 7 shows the estimated target shape using the proposed phase compensation algorithm. We see the estimation accuracy is improved without sacrificing the resolution.

6. Conclusions

High-resolution shape estimation algorithms utilize the information of carrier phase. The estimation accuracy degrades on a certain condition because the carrier phase depends on the target shape. We proposed a phase compensation algorithm for SEABED algorithm. We have clarified that phase compensation can be possible using a value ϕ which is calculated using a quasi wavefront and its 1st- and 2nd-order derivatives. We have proposed the phase compensation algorithm based on ϕ. The proposed phase compensation algorithm works well and estimates target surfaces accurately including its edge points.

REFERENCES

[1] D. Nahamoo, S. X. Pan and A. C. Kak, "Synthetic aparture diffraction tomography and its interpolation-free computer implementation," IEEE Trans. Sonics and Ultrasonics, Vol. 31, No. 4, pp. 218–229, 1984.
[2] M. B. Dobrin and C. H. Savit, Introduction to Geophysical Prospecting, Fourth Edition, McGraw-Hill, New York, 1988.
[3] J. V. Candy and C. Pichot, "Active microwave imaging : A model-based approach," IEEE Trans. Antennas Propagat., Vol. 39, No. 3, pp. 285–290, 1991.
[4] P. Chaturvedi and R. G. Plumb, "Electromagnetic imaging of underground targets using constrained optimization," IEEE Trans. Geosci. Remote Sensing, Vol. 33, No. 3, pp.551–561, 1995.
[5] T. Sato, K. Takeda, T. Nagamatsu, T. Wakayama, I. Kimura and T. Shinbo, "Automatic signal processing of front monitor radar for tunnelling machines," IEEE Trans. Geosci. Remote Sens., Vol. 35, No. 2, pp. 354–359, 1997.
[6] T. Sato, T. Wakayama and K. Takemura, "An imaging algorithm of objects embedded in a lossy dispersive medium for subsurface radar data processing," IEEE Trans. Geosci. Remote Sens., Vol. 38, No. 1, pp. 296–303, 2000.
[7] T. Takenaka, H. Jia and T. Tanaka, "Microwave imaging of an anisotropic cylindrical object by a forward-backward time-stepping method," IEICE Trans. Electron., Vol. E84-C, No. 12, pp. 1910–1916, 2001.
[8] T. Sakamoto and T. Sato, "A phase compensation algorithm for high-resolution pulse radar systems," IEICE Trans. Communications, (submitted).
[9] T. Sakamoto and T. Sato, "A target shape estimation algorithm for UWB pulse radar systems based on boundary scattering transform," IEICE Trans. Communications, 2004, (accepted for publication).
[10] G. L. James, Geometrical Theory of Diffraction for Electromagnetic Waves, IEE Electromagnetic waves series 1, Peter Peregrinus Ltd., UK, 1980.
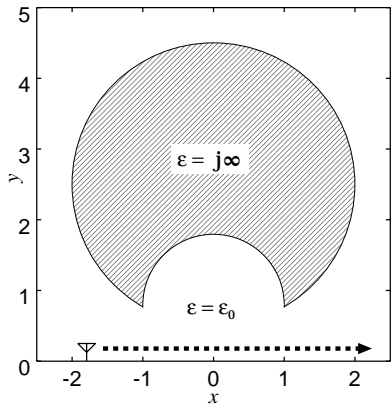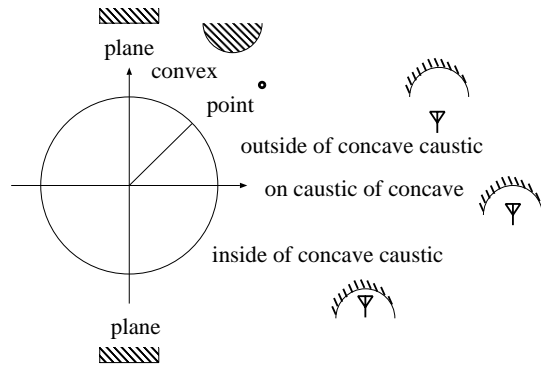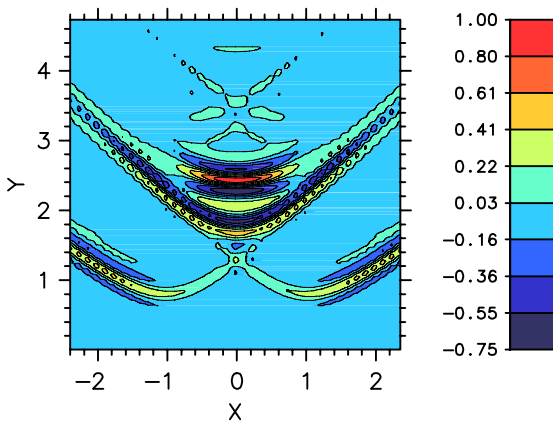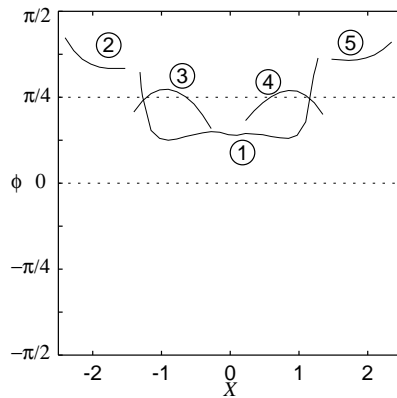
Fig. 1.   Target model.

Fig. 2.   Observed signal.
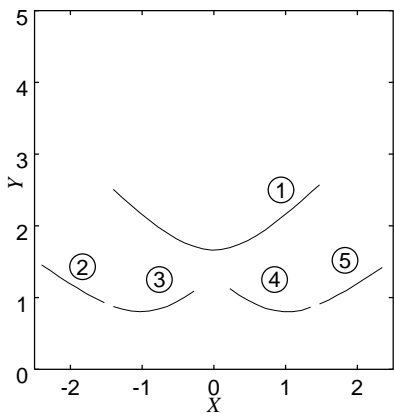
Fig. 3.   Extracted quasi wavefronts.

Fig. 4.   Estimated target shape using SEABED.

Fig. 5. ϕ and boundary shape.

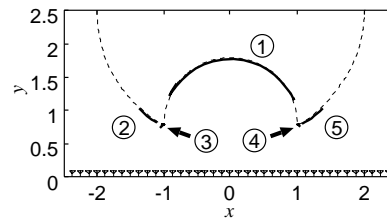Fig. 6. ϕ for each quasi wavefront.

Fig. 7.   Estimated target shape using the proposed phase compensation algorithm.